AGT

Algebraic & Geometric Topology

Volume 25 (2025)

An example of higher-dimensional Heegaard Floer homology

YIN TIAN
TIANYU YUAN

msp

msp

Algebraic & Geometric Topology **25**:3 (2025) 1877–1896
DOI: 10.2140/agt.2025.25.1877
Published: 20 June 2025

An example of higher-dimensional Heegaard Floer homology

YIN TIAN
TIANYU YUAN

We count pseudoholomorphic curves in the higher-dimensional Heegaard Floer homology of disjoint cotangent fibers of a two-dimensional disk. We show that the resulting algebra is isomorphic to the Hecke algebra associated to the symmetric group.

53D40; 53D10

1 Introduction

Many topological properties of a manifold M can be recovered from the symplectic geometry of its cotangent bundle T^*M. An example is the A_∞-equivalence between the wrapped Floer homology $\mathrm{CW}^*(T_q^*M)$ of a cotangent fiber and the space $C_{-*}(\Omega_q M)$ of chains on the based loop space of M, proved by Abbondandolo and Schwarz [1] and Abouzaid [2].

On the symplectic side, there is a generalization, the wrapped Floer homology $\mathrm{CW}^*\big(\bigsqcup_{i=1}^{\kappa} T_{q_i}^*M\big)$ of κ disjoint cotangent fibers in the framework of *higher-dimensional Heegaard Floer homology* (abbreviated HDHF) established by Colin, Honda and Tian [3]. It is related to the braid group of M on the topological side.

When $M=\Sigma$ is a real oriented surface, the HDHF was recently studied by Honda, Tian and Yuan [7]. Pick κ basepoints $\boldsymbol{q}=\{q_1,\dots,q_\kappa\}\subset\Sigma$. By definition, $\mathrm{CW}^*\big(\bigsqcup_i T_{q_i}^*\Sigma\big)$ is an A_∞ algebra over $\mathbb{Z}[[\hbar]]$, where $\hbar$ keeps track of the Euler characteristic of the holomorphic curves that are counted in the definition of the A_∞-operations. If Σ is not a two sphere, then $\mathrm{CW}^*\big(\bigsqcup_i T_{q_i}^*\Sigma\big)$ is supported in degree zero. Hence, it is isomorphic to its homology $\mathrm{HW}^*\big(\bigsqcup_i T_{q_i}^*\Sigma\big)$ as an ordinary algebra. The main result of [7] is that the algebra $\mathrm{HW}^*\big(\bigsqcup_i T_{q_i}^*\Sigma\big)$ is isomorphic to the *braid skein algebra* $\mathrm{BSk}_\kappa(\Sigma)$ of Σ, which was defined by Morton and Samuelson [9]. Roughly speaking, $\mathrm{BSk}_\kappa(\Sigma)$ is a quotient of the group algebra of the braid group of Σ by the *HOMFLY skein relation*, which is expressed in terms of $\hbar$. The skein relation has an explanation as holomorphic curve counting due to Ekholm and Shende [4]. This is one of the keys to build the bridge between $\mathrm{HW}^*\big(\bigsqcup_i T_{q_i}^*\Sigma\big)$ and $\mathrm{BSk}_\kappa(\Sigma)$.

Morton and Samuelson showed that $\mathrm{BSk}_\kappa(\Sigma)$ is isomorphic to the *double affine Hecke algebra* associated to $\mathfrak{gl}_\kappa$ when Σ is a torus. Based on this result, Honda, Tian and Yuan proved the isomorphisms between $\mathrm{HW}^*\big(\bigsqcup_i T_{q_i}^*\Sigma\big)$ and various Hecke algebras of type A for Σ being a disk, a cylinder or a torus.

Here we focus on the local case: $\Sigma = D^2$ is a disk. Let $\mathrm{End}(L^{\otimes\kappa})$ denote the algebra $\mathrm{HW}^*\big(\bigsqcup_i T^*_{q_i} D^2\big)$ throughout the paper. It is isomorphic to the finite Hecke algebra associated to the symmetric group S_κ over $\mathbb{Z}[[\hbar]]$; see [7]. The main result of this paper is to show that $\mathrm{End}(L^{\otimes\kappa})$ can be defined over $\mathbb{Z}[\hbar]$, and the isomorphism to the finite Hecke algebra still holds.

The reduction from $\mathbb{Z}[[\hbar]]$ to $\mathbb{Z}[\hbar]$ has two advantages regarding connections to other fields. The first one is topological. The HOMFLYPT polynomial of links takes values in the ring of Laurent polynomials of $\hbar$. This polynomial can be obtained from a trace function on the Hecke algebra; see Jones [8]. Note that the HOMFLYPT polynomial has a Floer-theoretic interpretation due to Ekholm and Shende [4]. It is interesting to look for connections between our curve counting for the Hecke algebra and theirs for the link invariant.

The second one is algebraic. We expect that the HDHF Fukaya category of $T^*\Sigma$ is related to the category of modules over the algebra $\mathrm{HW}^*\big(\bigsqcup_i T^*_{q_i}\Sigma\big)$. Representation theory over $\mathbb{Z}[[\hbar]]$ and $\mathbb{Z}[\hbar]$ could be different. Modules over $\mathbb{Z}[\hbar]$ or $\mathbb{Z}[q,q^{-1}]$ are commonly used in representation theory of various Hecke algebras.

We explicitly describe our main result in the following. The Floer generators of $\mathrm{End}(L^{\otimes\kappa})$ are tuples of intersection points between the cotangent fibers $T^*_{q_i} D^2$. They are in one-to-one correspondence to elements of the symmetric group S_κ. Let $T_w \in \mathrm{End}(L^{\otimes\kappa})$ denote the corresponding Floer generator for $w \in S_\kappa$.

For the Hecke algebra, we change the variable from q to $\hbar$ via $\hbar = q - q^{-1}$ for our purpose.

Definition 1.1 The Hecke algebra H_κ is a unital $\mathbb{Z}[\hbar]$-algebra generated by $\widetilde{T}_1, \dots, \widetilde{T}_{\kappa-1}$, with relations

$$\widetilde{T}_i^2 = 1 + \hbar\widetilde{T}_i, \qquad \widetilde{T}_i\widetilde{T}_j = \widetilde{T}_j\widetilde{T}_i \quad \text{for } |i-j|>1 \qquad \text{and} \qquad \widetilde{T}_i\widetilde{T}_{i+1}\widetilde{T}_i = \widetilde{T}_{i+1}\widetilde{T}_i\widetilde{T}_{i+1}.$$

It is known that the Hecke algebra H_κ is a free $\mathbb{Z}[\hbar]$-module with a basis $\widetilde{T}_w$ for $w \in S_\kappa$, called the *standard basis*. Here $\widetilde{T}_i = \widetilde{T}_{s_i}$ for the transposition $s_i = (i, i+1)$. There is a length function on S_κ defined by $l(w) = \min\{l \mid w = s_{i_1}\cdots s_{i_l}\}$. The basis $\widetilde{T}_w = \widetilde{T}_{i_1}\cdots\widetilde{T}_{i_l}$ if $w = s_{i_1}\cdots s_{i_l}$ is an expression of minimal length. Moreover, the algebra structure on H_κ is uniquely determined by

$$\widetilde{T}_i\widetilde{T}_w = \begin{cases} \widetilde{T}_{s_i w} & \text{if } l(s_i w) > l(w), \\ \widetilde{T}_{s_i w} + \hbar\widetilde{T}_w & \text{if } l(s_i w) < l(w). \end{cases} \tag{1-1}$$

Our main result is the following.

Theorem 1.2 *The HDHF homology* $\mathrm{End}(L^{\otimes\kappa})$ *is defined over* $\mathbb{Z}[\hbar]$. *Moreover, there is an isomorphism of unital algebras* $\phi\colon H_\kappa \to \mathrm{End}(L^{\otimes\kappa})$ *such that* $\phi(\widetilde{T}_w) = T_w$ *for* $w \in S_\kappa$.

In other words, we give a Floer-theoretic explanation of the standard basis of the Hecke algebra H_κ.

Unlike the method presented in [7], our proof takes a different approach by directly counting holomorphic curves in HDHF. Curve counting is in general a challenging task unless the ambient symplectic manifold is of real dimension two. We arrange the Lagrangian boundary conditions in a split form such that the curve counting problem reduces to the case of two copies of $\mathbb{C}$. Our strategy consists of two main steps:

(1) When $\kappa = 2$, we are able to show that there exists a nontrivial holomorphic disk, which corresponds to the $\hbar$ term in the quadratic relation of the Hecke algebra; see Lemma 3.5. To see this curve, in each copy of $\mathbb{C}$, the counting is combinatorial and provides a relative homology class within the moduli space of a hexagon. The nontrivial intersection number of two relative classes from the two copies of $\mathbb{C}$ then shows the existence of such a curve.

(2) To prove the Hecke relation holds in HDHF in general, we proceed by induction on κ. By stretching the Lagrangians in a certain order, the corresponding family of holomorphic curves degenerates into several pieces due to Gromov compactness. The degenerated curves live in the moduli space associated to $\kappa' = \kappa - 1$ or $\kappa - 2$. Therefore we can do induction on κ.

Further directions (1) It is natural to ask whether the HDHF homology $\mathrm{End}\big(\bigsqcup_i T^*_{q_i}\Sigma\big)$ of disjoint fibers of $T^*\Sigma$ can be defined over $\mathbb{Z}[\hbar]$ for a general surface Σ. We hope to generalize our result from local to global by using some sheaf-theoretic techniques, for instance those of Ganatra, Pardon and Shende [6]. The idea is to establish a pushout diagram so that $\mathrm{End}\big(\bigsqcup_i T^*_{q_i}\Sigma\big)$ can be realized as a homotopy colimit of the local pieces which is defined over $\mathbb{Z}[\hbar]$.

(2) It is interesting to explain the geometric meaning of the change of variables $\hbar = q - q^{-1}$. Note that the *canonical basis* of the Hecke algebra is defined over $\mathbb{Z}[q, q^{-1}]$. We will express the canonical basis via HDHF in an upcoming paper.

(3) When the symplectic manifold is of dimension greater than four, a similar technique can be used to compute the local case T^*D^m for $m > 2$. In this case, we expect that the HDHF homology $\mathrm{HW}^*\big(\bigsqcup_i T^*_{q_i}D^m\big)$ is a nontrivial A_∞ algebra. Its nontrivial higher A_∞ relation can be viewed as a generalization of the quadratic relation in the Hecke algebra.

Acknowledgements The authors thank Ko Honda for numerous ideas and suggestions. Tian is supported by NSFC 11971256. Yuan is supported by China Postdoctoral Science Foundation 2023T160002.

2 Preliminaries

We first specify the ambient manifold and Lagrangian submanifolds of interest. For convenience of curve counting, we set $D^2 = I_1 \times I_2$ with $I_1 = I_2 = [0, 1]$, which is topologically the same as the unit disk. Let $X = T^*D^2 = T^*I_1 \times T^*I_2$ be the total space of the cotangent bundle of D^2.

Consider the canonical Liouville form θ on T^*D^2, which induces a contact manifold structure at the infinity of (T^*D^2, θ). For a Lagrangian $L \subset T^*D^2$, denote its boundary at infinity by $\partial_\infty L$. An isotopy of Lagrangians L_t in T^*D^2 is called *positive* if $\alpha(\partial_t \partial_\infty L_t) > 0$ for all t. Let $T^*_v D^2 = T^*D^2|_{\partial D^2}$ be the vertical boundary of T^*D^2 over ∂D^2. We require that any isotopy L_t cannot cross $T^*_v D^2$. A positive isotopy is also called a "partially wrapping". For the details of partially wrapped Fukaya categories, we refer to [10] by Sylvan and [5] by Ganatra, Shende, and Pardon.

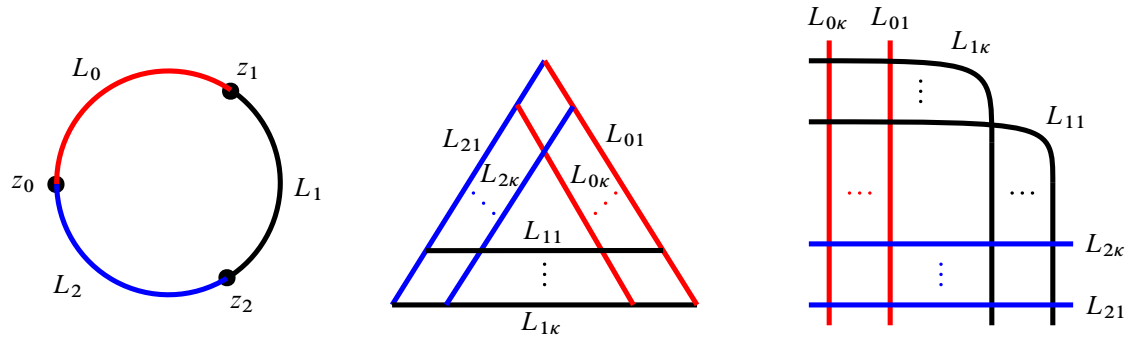

Figure 1: Left: D_3, the A_∞ base direction. Center: the Lagrangians in the T^*I_1 direction. Right: the Lagrangians in the T^*I_2 direction.

We next consider the generalization to wrapped HDHF. Pick κ disjoint basepoints $\boldsymbol{q} = \{q_1, \dots, q_\kappa\} \subset D^2 \backslash \partial D^2$ and consider the κ cotangent fibers $L_{0i} = T^*_{q_i} D$ for $i = 1, \dots, \kappa$. We define $\mathcal{L}_0 = \{L_{01}, \dots, L_{0\kappa}\}$. An isotopy of a κ-tuple of Lagrangians $\mathcal{L}_t = \{L_{t1}, \dots, L_{t\kappa}\}$ is called *positive* if $\alpha(\partial_t \partial_\infty L_{ti}) > 0$ for all $i = 1, \dots, \kappa$ and all t. For a pair of κ-tuples of Lagrangians $\mathcal{A}$ and $\mathcal{B}$, we write $\mathcal{A} \rightsquigarrow \mathcal{B}$ if there is an positive isotopy from $\mathcal{A}$ to $\mathcal{B}$.

We then perform positive wrapping on $\mathcal{L}_0$ to get $\mathcal{L}_j = \{L_{j1}, \dots, L_{j\kappa}\}$ for $j = 1, 2$. Specifically, we put $\mathcal{L}_0$, $\mathcal{L}_1$ and $\mathcal{L}_2$ in the position as in Figure 1, center and right, which represent the T^*I_1-direction and T^*I_2-direction, respectively. It is easy to check that

$$\mathcal{L}_0 \rightsquigarrow \mathcal{L}_1 \rightsquigarrow \mathcal{L}_2.$$

The HDHF cochain complex $\mathrm{CF}^*(\mathcal{L}_i, \mathcal{L}_j)$ for $i < j$ is defined as the free abelian group generated by κ-tuples of intersection points between $\mathcal{L}_i$ and $\mathcal{L}_j$ over $\mathbb{Z}[[\hbar]]$. By definition, $\mathrm{CF}^*(\mathcal{L}_i, \mathcal{L}_j)$ is an A_∞-algebra. We refer the reader to [7] for details of the definition of HDHF in this case.

There is an absolute grading on $\mathrm{CF}^*(\mathcal{L}_i, \mathcal{L}_j)$ and the degree is supported at zero by [7, Proposition 2.9]. Hence, its homology $\mathrm{HF}^*(\mathcal{L}_i, \mathcal{L}_j)$ is an ordinary algebra over $\mathbb{Z}[[\hbar]]$. We denote it by $\mathrm{End}(L^{\otimes\kappa})$.

Remark 2.1 Strictly speaking, the algebra structure of $\mathrm{End}(L^{\otimes\kappa})$ is given by the composition map

$$\mu^2 \colon \mathrm{HF}^*(\mathcal{L}_1, \mathcal{L}_2) \otimes \mathrm{HF}^*(\mathcal{L}_0, \mathcal{L}_1) \to \mathrm{HF}^*(\mathcal{L}_0, \mathcal{L}_2),$$

together with the continuation maps

$$c_{12} \circ - \colon \mathrm{HF}^*(\mathcal{L}_0, \mathcal{L}_1) \xrightarrow{\sim} \mathrm{HF}^*(\mathcal{L}_0, \mathcal{L}_2), \tag{2-1}$$

$$- \circ c_{01} \colon \mathrm{HF}^*(\mathcal{L}_1, \mathcal{L}_2) \xrightarrow{\sim} \mathrm{HF}^*(\mathcal{L}_0, \mathcal{L}_2), \tag{2-2}$$

where $c_{12} \in \mathrm{HF}^*(\mathcal{L}_1, \mathcal{L}_2)$ and $c_{01} \in \mathrm{HF}^*(\mathcal{L}_0, \mathcal{L}_1)$ are two specific generators, both denoted by T_{id} in Section 3. In this way, we have defined the algebra structure on $\mathrm{HF}^*(\mathcal{L}_0, \mathcal{L}_2)$.

In order to compute the algebra $\mathrm{End}(L^{\otimes\kappa})$, we need to explicitly compute the maps (2-1) and (2-2). It is then necessary that (2-1) and (2-2) are indeed identity maps (with respect to some choice of basis of

Floer generators) instead of just isomorphisms. With our specific choice of wrapping, we can show that the continuation maps preserve the Floer generators for different $\mathrm{HF}^*(\mathcal{L}_i, \mathcal{L}_j)$ with $i < j$. In other words, we show that T_{id} behaves as the identity of the algebra; see Proposition 3.1.

Remark 2.2 We fix the special wrapping of $\mathcal{L}_0$, $\mathcal{L}_1$ and $\mathcal{L}_2$, which is crucial for our counting of curves. We remark that the algebraic count is invariant under compactly supported perturbation of Lagrangians; see [3, Section 6]. Indeed, we can show that the specific choice of Figure 1, right, is only for computing convenience, and the count remains the same if we rearrange Figure 1, right, eg to be like Figure 1, center. However, currently we do not know whether the same holds if we perturb the Lagrangians at infinity without keeping the Lagrangians in a product form.

We describe the μ^2-composition map of $\mathrm{End}(L^{\otimes\kappa})$ in the following. We set $\widehat{X} = D_3 \times X$ as the target manifold, where D_3 is the unit disk with three boundary punctures, and refer to it as the "A_∞ base direction". Let z_0, z_1 and z_2 be the boundary punctures of D_3 and let α_0, α_1 and α_2 be the boundary arcs. We extend $\mathcal{L}_i$ to the D_3 direction by setting $\widehat{\mathcal{L}}_i = \alpha_i \times \mathcal{L}_i$ and $\widehat{L}_{ij} = \alpha_i \times L_{ij}$ for $i = 0, 1, 2$ and $j = 1, \dots, \kappa$, which are Lagrangian submanifolds of $\widehat{X}$.

For $i = 1, 2$, let $\boldsymbol{y}_i = \{y_{i1}, \dots, y_{i\kappa}\}$ be a tuple of intersection points $y_{ij} \in \widehat{L}_{(i-1)j} \cap \widehat{L}_{ij'}$, where $\{1', \dots, \kappa'\}$ is some permutation of $\{1, \dots, \kappa\}$. Let J be a small generic perturbation of $J_{D_3} \times J_1 \times J_2$, where J_{D_3}, J_1 and J_2 are the standard complex structures on D_3, T^*I_1 and T^*I_2, viewed as subsets of $\mathbb{C}$. Let $\mathcal{M}(\boldsymbol{y}_1, \boldsymbol{y}_2, \boldsymbol{y}_0)$ be the moduli space of maps

$$u\colon (\dot{F}, j) \to (\widehat{X}, J), \tag{2-3}$$

where (F, j) is a compact Riemann surface with boundary, $\boldsymbol{p}_i$ are disjoint tuples of boundary punctures of F for $i = 0, 1, 2$, and $\dot{F} = F \setminus \bigcup_i \boldsymbol{p}_i$. The map u satisfies

$$\begin{cases} du \circ j = J \circ du, \\ \text{each component of } \partial\dot{F} \text{ is mapped to a unique } \widehat{L}_{ij}, \\ \pi_X \circ u \text{ tends to } \boldsymbol{y}_i \text{ as } s_i \to +\infty \text{ for } i = 1, \dots, m, \\ \pi_X \circ u \text{ tends to } \boldsymbol{y}_0 \text{ as } s_0 \to -\infty, \\ \pi_{D_3} \circ u \text{ is a } \kappa\text{-fold branched cover of } D_3, \end{cases} \tag{2-4}$$

where the third condition means that $\pi_X \circ u$ maps the neighborhoods of the punctures of $\boldsymbol{p}_i$ asymptotically to the Reeb chords of $\boldsymbol{y}_i$ for $i = 1, \dots, m$ at the positive ends. The fourth condition is similar.

The μ^2-composition map of $\mathrm{End}(L^{\otimes\kappa})$ is then defined as

$$\mu^2(\boldsymbol{y}_1, \boldsymbol{y}_2) = \sum_{\boldsymbol{y}_0, \chi \le \kappa} \#\mathcal{M}^{\mathrm{ind}=0,\chi}(\boldsymbol{y}_1, \boldsymbol{y}_2, \boldsymbol{y}_0) \cdot \hbar^{\kappa-\chi} \cdot \boldsymbol{y}_0, \tag{2-5}$$

where the superscript "ind" denotes the Fredholm index and "χ" denotes the Euler characteristic of F; the symbol # denotes the signed count of the corresponding moduli space.

A choice of spin structures on the Lagrangians determines a canonical orientation of the moduli space. The Lagrangian in our case is the cotangent fiber, which is topologically $\mathbb{R}^2$. So there is a unique spin structure. We omit the details about the orientation, and refer the reader to [3, Section 3].

3 The case of $\kappa = 2$

In this section we compute $\mathrm{End}(L^{\otimes 2})$ as a model case. The general case will be discussed in Section 4.

For $0 \le i < j \le 2$, there are two Floer generators of $\mathrm{CF}^*(\mathcal{L}_i, \mathcal{L}_j)$: T_{id} and T_1, where $T_{\mathrm{id}} = (q_1, q_2)$ with $q_1 \in L_{i1} \cap L_{j1}$ and $q_2 \in L_{i2} \cap L_{j2}$, and $T_1 = (q_1, q_2)$ with $q_1 \in L_{i1} \cap L_{j2}$ and $q_2 \in L_{i2} \cap L_{j1}$. The main result of this section is the following:

Proposition 3.1 *The multiplication on* $\mathrm{End}(L^{\otimes 2})$ *is given by*

$$T_{\mathrm{id}} \cdot T_{\mathrm{id}} = T_{\mathrm{id}}, \quad T_{\mathrm{id}} \cdot T_1 = T_1, \quad T_1 \cdot T_{\mathrm{id}} = T_1 \quad \text{and} \quad T_1 \cdot T_1 = 1 + \hbar T_1.$$

Hence Theorem 1.2 holds for $\kappa = 2$.

The proof of this proposition occupies the rest of the section. We directly compute the moduli spaces. There are trivial curves with $\chi = 2$ accounting for the $\hbar^0$ terms in the multiplication. We show that $\mathcal{M}_J^{\chi<2}(y_1, y_2, y_0) = \varnothing$ for almost all cases except that $\mathcal{M}_J^{\chi=1}(T_1, T_1, T_1) \neq \varnothing$ accounting for the $\hbar^1$ term in $T_1 \cdot T_1$. The main strategy to prove the nonexistence of curves is to stretch the Lagrangians in the T^*I_1-direction and apply Gromov compactness.

For later use, we make the following conventions:

- We denote the length of the line segment of $L_{1\kappa}$ in the I_1-direction by d; see Figure 1, center.
- For $q \in X$, we denote its projection in the T^*I_1 (resp. T^*I_2) direction by q' (resp. q'').
- We denote the line segment between q_1 and q_2 by $(q_1 q_2)$.
- When plotting figures, we denote the intersections q_i by i.
- When taking the limit, we denote the degenerated domain by $\dot{F}'$ and its irreducible component containing $\{p_1, p_2, \dots\}$ by $\dot{F}'_{(12\dots)}$.

Lemma 3.2 $$T_{\mathrm{id}} \cdot T_{\mathrm{id}} = T_{\mathrm{id}}.$$

Proof We first show that

$$\#\mathcal{M}^{\chi}(T_{\mathrm{id}}, T_{\mathrm{id}}, T_{\mathrm{id}}) = \begin{cases} 1 & \text{if } \chi = 2, \\ 0 & \text{if } \chi < 2. \end{cases} \tag{3-1}$$

The Floer generators are shown in Figure 2.

If $\chi = 2$, there is a unique trivial holomorphic curve consisting of two disks. So $\#\mathcal{M}^{\chi=2}(T_{\mathrm{id}}, T_{\mathrm{id}}, T_{\mathrm{id}}) = 1$.

If $\chi < 2$, let $d \to 0$, ie let q_1' and q_2' get closer. In the limit, since there are no slit or branch points separating q_1' and q_2', $\dot{F}'_{(12)}$ bubbles off as a triangle with vertices $\{p_1, p_2, p_a\}$, where $\{p_a\}$ is a boundary

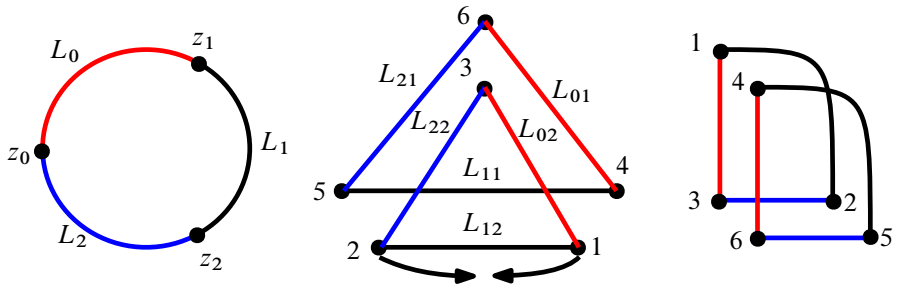

Figure 2: Generators for $\mathcal{M}(T_{\mathrm{id}}, T_{\mathrm{id}}, T_{\mathrm{id}})$.

nodal point. The projection of $\dot{F}'_{(12)}$ under $\pi_{T^*I_2} \circ u$ is a homeomorphism to the triangle with vertices $\{q''_1, q''_2, q''_3\}$. Hence the projection of $\dot{F}'_{(3)}$ under $\pi_{T^*I_2} \circ u$ is a constant map to q''_3. Since $\pi_{T^*I_2} \circ u$ is of degree zero or one near q''_3, the image $\pi_{T^*I_2} \circ u(\dot{F} \setminus (\dot{F}'_{(12)} \cup \dot{F}'_{(3)}))$ is disjoint from q''_3. So $\dot{F}'_{(12)} \cup \dot{F}'_{(3)}$ is a connected component of $\dot{F}'$. Therefore $\dot{F}$ consists of two components before the degeneration, which are homeomorphically mapped to the triangles $\{q''_1, q''_2, q''_3\}$ and $\{q''_4, q''_5, q''_6\}$ under $\pi_{T^*I_2} \circ u$, respectively. So $\chi = 2$, which is a contradiction. We conclude that $\#\mathcal{M}^{\chi}(T_{\mathrm{id}}, T_{\mathrm{id}}, T_{\mathrm{id}}) = 0$ if $\chi < 2$.

We next show that $\#\mathcal{M}(T_{\mathrm{id}}, T_{\mathrm{id}}, T_1) = 0$. The generators are shown in Figure 3. As $d \to 0$, $\dot{F}'_{(12)}$ bubbles off as a triangle with vertices $\{p_1, p_2, p_a\}$, where $p_a \in \dot{F}'$ is a nodal point. Denote the union of irreducible components of $\dot{F}'$ containing the preimage of the dashed lines in the T^*I_1-direction by $\dot{F}'_{\mathrm{dash}}$. Since p_3, p_6 and p_a are mapped to z_0 under $\pi_{D_3} \circ u$ in the limit, the preimages of the dashed lines are also mapped to z_0. Hence $\dot{F}'_{\mathrm{dash}}$ is mapped to the constant point z_0 under $\pi_{D_3} \circ u$. Since $(q'_5 q'_6)$ cannot be separated by slits, $q'_5 \in \dot{F}'_{\mathrm{dash}}$ and $\pi_{D_3} \circ u(q'_5) = z_0$. This contradicts with the fact that $\pi_{D_3} \circ u(q'_5) = z_2$. Therefore $\mathcal{M}(T_{\mathrm{id}}, T_{\mathrm{id}}, T_1) = \varnothing$. □

Lemma 3.3 $$T_{\mathrm{id}} \cdot T_1 = T_1.$$

Proof First we show that

$$\#\mathcal{M}^{\chi}(T_{\mathrm{id}}, T_1, T_1) = \begin{cases} 1 & \text{if } \chi = 2, \\ 0 & \text{if } \chi < 2. \end{cases} \tag{3-2}$$

The generators are shown in Figure 4.

If $\chi = 2$, there is a unique trivial holomorphic curve consisting of two disks. So $\#\mathcal{M}^{\chi=2}(T_{\mathrm{id}}, T_1, T_1) = 1$.

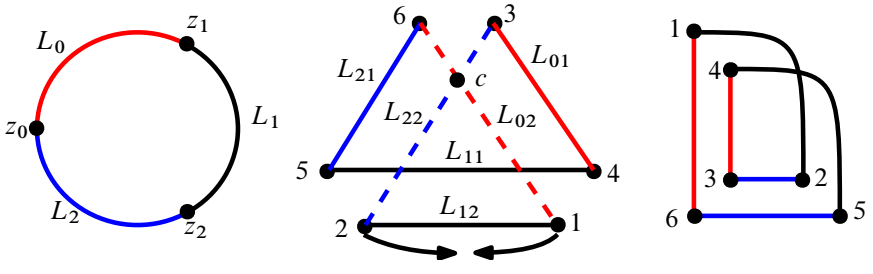

Figure 3: Generators for $\mathcal{M}(T_{\mathrm{id}}, T_{\mathrm{id}}, T_1)$.

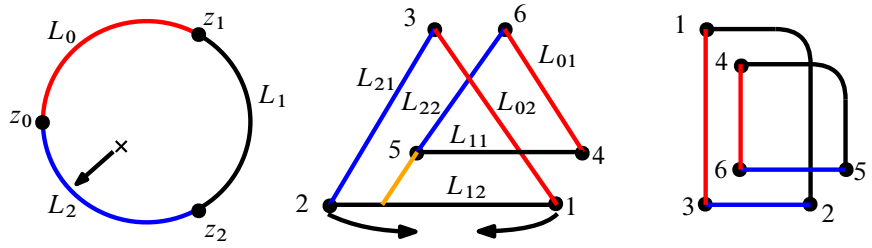

Figure 4: Generators for $\mathcal{M}(T_{\mathrm{id}}, T_1, T_1)$.

If $\chi < 2$, as $d \to 0$, there are two cases:

- If the orange slit extending $(q_6' q_5')$ is not long, then $\dot{F}'_{(12)}$ bubbles off as a triangle with vertices $\{p_1, p_2, p_a\}$. The remaining proof is the same as that of $\#\mathcal{M}^{\chi}(T_{\mathrm{id}}, T_{\mathrm{id}}, T_{\mathrm{id}}) = 0$ for $\chi < 2$ in Lemma 3.2. Hence, the limiting curve does not exist.

- If the orange slit extending $(q_6' q_5')$ is long, then there is a branch point approaching the interior of L_2 in the D_3-direction (as in the left of Figure 4). In the limit, the preimage of the branch point on the domain tends to some nodal point p_n such that $\pi_{D_3} \circ u(p_n) \in L_2$. This implies that $\pi_{T^*I_2} \circ u(p_n) \in L_{21} \cap L_{22}$. This contradicts with the fact that $L_{21} \cap L_{22} = \varnothing$ in the T^*I_2-direction.

Next we show that $\#\mathcal{M}^{\chi}(T_{\mathrm{id}}, T_1, T_{\mathrm{id}}) = 0$ for $\chi \leq 2$. The generators are shown in Figure 5. As $d \to 0$, $\dot{F}'_{(12)}$ bubbles off as a triangle $\{p_1, p_2, p_a\}$. Then p_a should be mapped to the intersection of the extension of the line segments $(q_1'' q_6'')$ and $(q_2'' q_3'')$. But this is impossible since the degree of the projection $\pi_{T^*I_2} \circ u$ is zero near the intersection. □

Similar arguments will be used in the proofs of Propositions 4.1 and 4.2. In general, $\dot{F}'_{(12)}$ always bubbles off as a triangle as $d \to 0$. Here q_1' and q_2' are on the bottom Lagrangian $L_{1\kappa}$ in the T^*I_1-direction. We then analyze the remaining irreducible components of $\dot{F}'$ and reduce the problem to simpler cases.

Lemma 3.4 $T_1 \cdot T_{\mathrm{id}} = T_1$.

Proof This is similar to the proof of Lemma 3.3. □

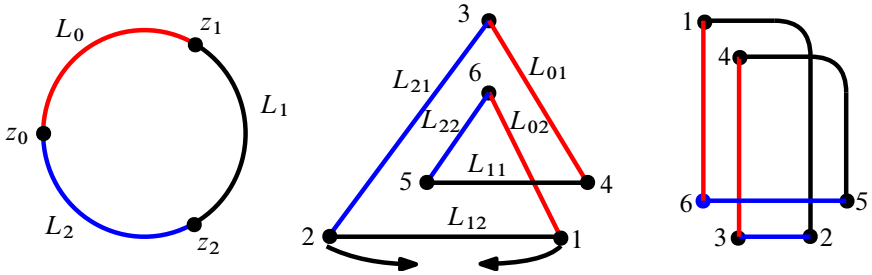

Figure 5: Generators for $\mathcal{M}(T_{\mathrm{id}}, T_1, T_{\mathrm{id}})$.

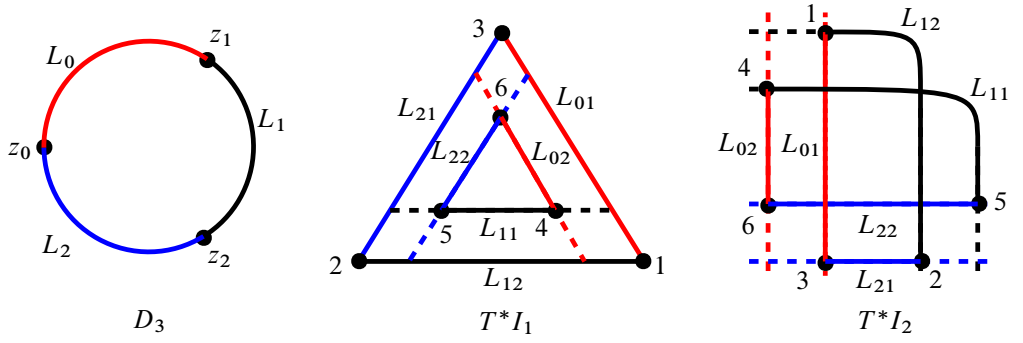

Figure 6: Generators for $\mathcal{M}(T_1, T_1, T_{\mathrm{id}})$.

Lemma 3.5 $$T_1 \cdot T_1 = T_{\mathrm{id}} + \hbar T_1.$$

Proof We first show that

$$\#\mathcal{M}^{\chi}(T_1, T_1, T_{\mathrm{id}}) = \begin{cases} 1 & \text{if } \chi = 2, \\ 0 & \text{if } \chi < 2. \end{cases} \tag{3-3}$$

The generators are shown in Figure 6.

If $\chi = 2$, there is a unique trivial holomorphic curve consisting of two disks, so $\#\mathcal{M}^{\chi=2}(T_1, T_1, T_{\mathrm{id}}) = 1$.

If $\chi < 2$, then $\dot{F}'_{(12)}$ bubbles off as a triangle as $d \to 0$. The projection of $\dot{F}'_{(12)}$ under $\pi_{T^*I_2} \circ u$ is a homeomorphism to the triangle $\{q''_1, q''_2, q''_3\}$. Hence the projection of $\dot{F}'_{(3)}$ under $\pi_{T^*I_2} \circ u$ is the constant map to q''_3. Since $\pi_{T^*I_2} \circ u$ is of degree zero or one near q''_3, the image of $\pi_{T^*I_2} \circ u(\dot{F} \setminus (\dot{F}'_{(12)} \cup \dot{F}'_{(3)}))$ is disjoint from q''_3. It follows that $\dot{F}'_{(12)} \cup \dot{F}'_{(3)}$ is a connected component of $\dot{F}'$. Therefore $\dot{F}$ consists of two components before the degeneration, which are homeomorphically mapped to the triangles $\{q''_1, q''_2, q''_3\}$ and $\{q''_4, q''_5, q''_6\}$ under $\pi_{T^*I_2} \circ u$, respectively. So $\chi = 2$, which is a contradiction.

We next show that

$$\#\mathcal{M}^{\chi}(T_1, T_1, T_1) = \begin{cases} 1 & \text{if } \chi = 1, \\ 0 & \text{if } \chi \neq 1. \end{cases} \tag{3-4}$$

The generators are shown in Figure 7.

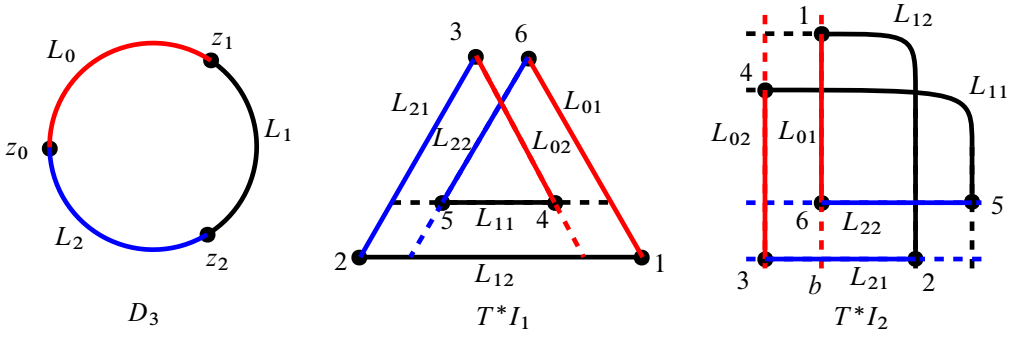

Figure 7: Generators for $\mathcal{M}(T_1, T_1, T_1)$.

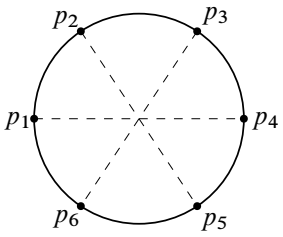

Figure 8: A disk $\dot{F} = D_6$ which satisfies the involution condition.

We denote the moduli space of domain $(\dot{F}, j)$ by $\mathcal{M}(\dot{F})$. By the Riemann–Roch formula, $\dim \mathcal{M}(\dot{F}) = 3(\kappa - \chi)$. Consider the moduli space of pseudoholomorphic maps from $(\dot{F}, j)$ to each direction D_3, T^*I_1 and T^*I_2, denoted by $\mathcal{M}(D_3)$, $\mathcal{M}(T^*I_1)$ and $\mathcal{M}(T^*I_2)$, respectively. The index formula says

$$\dim \mathcal{M}(D_3) = \dim \mathcal{M}(T^*I_1) = \dim \mathcal{M}(T^*I_2) = 2(\kappa - \chi),$$

for generic J. We have

$$\mathcal{M}(T_1, T_1, T_1) = \mathcal{M}(D_3) \cap \mathcal{M}(T^*I_1) \cap \mathcal{M}(T^*I_2). \tag{3-5}$$

Our main strategy to count curves in $\mathcal{M}(T_1, T_1, T_1)$ is computing the moduli space for each direction and then counting their intersection number.

The moduli space of curves restricted to each direction has an explicit parametrization. For example, $\pi_{D_3} \circ u$ from $\dot{F}$ to D_3 is a κ-fold branched cover, and its restriction to $\partial \dot{F}$ is a κ-fold cover over S^1. Generically, $\pi_{D_3} \circ u$ is parametrized by the positions of $\kappa - \chi$ double branch points on $\dot{F}$ over D_3.

In the case $\kappa = 2$ and $\chi = 1$, $\dot{F} = D_6$ is a disk with six boundary punctures. The moduli space of $(\dot{F}, j)$ is

$$\mathcal{M}(\dot{F}) \simeq \mathbb{R}^3.$$

Then we consider the cut-out moduli space $\mathcal{M}(D_3)$, viewed as a subset of $\mathcal{M}(\dot{F})$. The deck transformation of $\pi_{D_3} \circ u$ imposes an involution condition on $\dot{F}$. In other words, we require that $\{p_i, p_{i+3}\}$ lie on a diameter for $i = 1, 2, 3$ after some fractional linear transformation. Therefore,

$$\mathcal{M}(D_3) \simeq \mathbb{R}^2.$$

The moduli space $\mathcal{M}(D_3)$ admits a compactification $\overline{\mathcal{M}}(D_3)$, which is described in Figure 9.

We first consider $\partial \mathcal{M}(D_3) \cap \mathcal{M}(T^*I_1)$; see Figure 7, center. A map in $\mathcal{M}(T^*I_1)$ may have a double branch point inside the inner region with degree two. As the branch point touches the boundary of the inner region, it is replaced by a slit with two switch points along the Lagrangians. Since we are interested in $\partial \mathcal{M}(D_3)$, the bubbling behavior in Figure 9 requires the slit to be very long, so that some switch point meets another Lagrangian. The involution condition further requires that such switch points come in pairs. We conclude that $\partial \mathcal{M}(D_3) \cap \mathcal{M}(T^*I_1)$ consists of two points: one passes q_5' to its left extending the line segment $(q_4'q_5')$ and downwards extending $(q_6'q_5')$; the other passes p_4 to its right extending $(q_5'q_4')$ and downwards extending $(q_3'q_4')$. The two points are depicted as the two circles on the boundary of the hexagon in Figure 10.

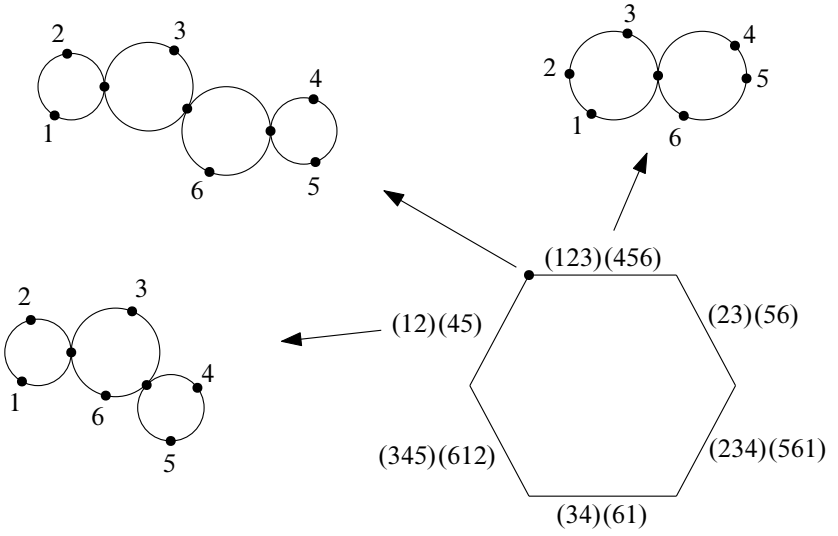

Figure 9: The compactified moduli space $\overline{\mathcal{M}}(D_3)$ is described by the hexagon. The index i stands for $p_i \in \partial \dot{F}$. The indices inside brackets describe the bubbling behavior, eg (12)(45) means p_1 is close to p_2 and p_4 is close to p_5. The involution condition is preserved on boundary strata, eg the cross ratio of the two bubble disks on the stratum (123)(456) are the same.

For $\partial\mathcal{M}(D_3) \cap \mathcal{M}(T^*I_2)$, see the Figure 7, right. Similar to the previous paragraph, the degeneration of D_6 requires the existence of long slits. There are two curves: one with a slit passing q_6'' to its left and downwards; the other lies on the Lagrangian $(q_1''q_2'')$ or $(q_4''q_5'')$ with one switch point meeting the intersection point $(q_1''q_2'') \cap (q_4''q_5'')$. The two curves are depicted as the dots on the hexagon in Figure 10.

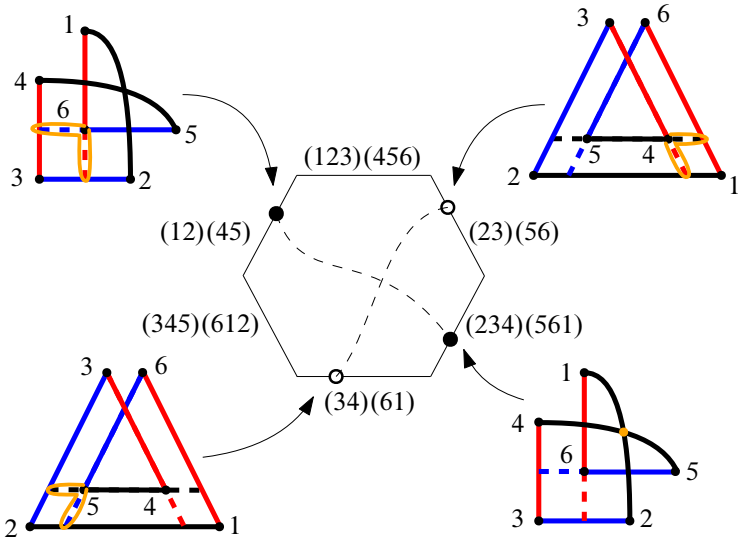

Figure 10: The orange arcs in the pictures outside the hexagon represent slits. The intersection of the two dashed arcs inside the hexagon represents a curve in $\mathcal{M}(D_3) \cap \mathcal{M}(T^*I_1) \cap \mathcal{M}(T^*I_2)$.

The relative position of dots and circles on $\partial\mathcal{M}(D_3)$ indicate $\mathcal{M}(D_3)\cap\mathcal{M}(T^*I_1)$ and $\mathcal{M}(D_3)\cap\mathcal{M}(T^*I_2)$ have intersection of algebraic count one inside $\mathcal{M}(D_3)$. Thus,

$$\#\mathcal{M}^{\chi=1}(T_1,T_1,T_1)=\#\mathcal{M}(D_3)\cap\mathcal{M}(T^*I_1)\cap\mathcal{M}(T^*I_2)=1. \tag{3-6}$$

If $\chi\neq 1$, we show that $\#\mathcal{M}^{\chi}(T_1,T_1,T_1)=0$. As $d\to 0$, $\dot{F}'_{(12)}$ bubbles off as a triangle. Since the projection of $\dot{F}'\backslash\dot{F}'_{(12)}$ to T^*I_2 is of degree one to its image (the polygon composed of $\{q''_3,q''_4,q''_5,q''_6,q''_b\}$ in Figure 7), the domain before degeneration has to be a disk. This contradicts with the fact that $\chi\neq 1$. □

The counting in (3-6) is essentially the only case where a nontrivial curve exists in our direct computation. It corresponds to the deformation $\widetilde{T}_i^2=1+\hbar\widetilde{T}_i$ from the symmetric group to the Hecke algebra.

4 The general case

In this section, we compute $\mathrm{End}(L^{\otimes\kappa})$ by induction on κ. Recall that $\mathrm{End}(L^{\otimes\kappa})$ is freely generated by $T_w=\{y_1,\dots,y_\kappa\}$, where $y_j\in L_{0j}\cap L_{1w(j)}$ and $w\in S_\kappa$ is viewed as a permutation. We compute $T_{w_1}\cdot T_{w_2}$ for $w_1,w_2\in S_\kappa$ by a case-by-case discussion depending on how w_1 acts on the last one or two elements of $\{1,\dots,\kappa\}$.

The first case is when w_1 fixes the last element. The schematic picture is shown in Figure 11. The following proposition is a generalization of Lemmas 3.2 and 3.3:

Proposition 4.1 *For $w_1,w_2,w_3\in S_\kappa$, suppose $w_1=w'_1$ and $w_2=w'_2s_{\kappa-1}s_{\kappa-2}\cdots s_{\kappa-m}$, where $w'_1,w'_2\in S_{\kappa-1}$ and $m\geq 0$. We have*

$$\#\mathcal{M}^{\chi}(T_{w_1},T_{w_2},T_{w_3})=\begin{cases}\#\mathcal{M}^{\chi-1}(T_{w'_1},T_{w'_2},T_{w'_3}) & \text{if } w_3=w'_3s_{\kappa-1}s_{\kappa-2}\cdots s_{\kappa-m},\\ 0 & \text{otherwise,}\end{cases}$$

where $w'_3\in S_{\kappa-1}$.

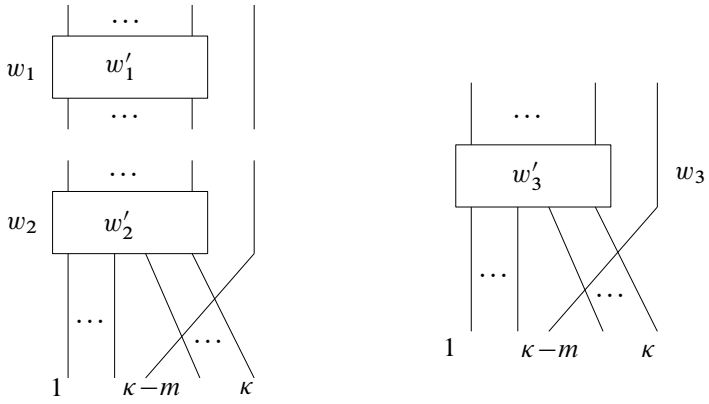

Figure 11: The case for Proposition 4.1.

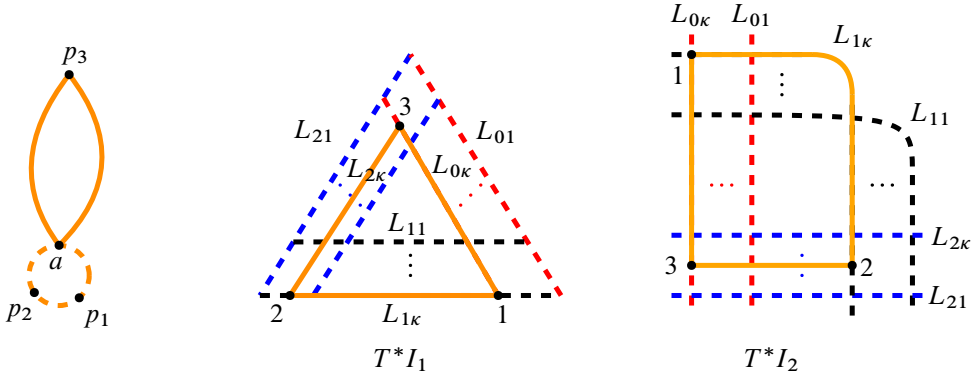

Figure 12: The case $t = \kappa - m$.

Proof Suppose that the strand of w_3 starting from the position κ ends on the position t; see Figure 11, right. Here, we are reading the picture for w_3 from top to bottom. We consider the following three cases depending on t:

(1) $(t = \kappa - m)$ Let $w_3 = w_3' s_{\kappa-1} s_{\kappa-2} \cdots s_{\kappa-m}$ for $w_3' \in S_{\kappa-1}$. This case is shown in Figure 12. The last vertical strand of w_1 in Figure 11 corresponds to p_1 in Figure 12. As $d \to 0$, $\dot{F}'_{(12)}$ bubbles off as a triangle with vertices $\{p_1, p_2, p_a\}$. The image of $\dot{F}'_{(12)}$ in the T^*I_2-direction is the orange triangle and the image of $\dot{F}'_{(3)}$ is the constant point q_3''. Since $\pi_{T^*I_2} \circ u$ is of degree zero or one near q_3'', the image $\pi_{T^*I_2} \circ u(\dot{F} \setminus (\dot{F}'_{(12)} \cup \dot{F}'_{(3)}))$ is disjoint from q_3''. This implies that $\dot{F}'_{(12)} \cup \dot{F}'_{(3)}$ is a connected component of $\dot{F}'$. Therefore $\dot{F}_{(123)}$ is a connected component of $\dot{F}$ before the degeneration, and it is mapped homeomorphically to the triangle $\{q_1'', q_2'', q_3''\}$ under $\pi_{T^*I_2} \circ u$. After removing the component $\dot{F}_{(123)}$, we see that $\#\mathcal{M}^{\chi}(T_{w_1}, T_{w_2}, T_{w_3}) = \#\mathcal{M}^{\chi-1}(T_{w_1'}, T_{w_2'}, T_{w_3'})$.

(2) $(t > \kappa - m)$ This case is shown in Figure 13. As $d \to 0$, $\dot{F}'_{(12)}$ bubbles off as a triangle with vertices $\{p_1, p_2, p_a\}$. There is a vertex p_b in the component $\dot{F}'_{(3)}$ which is adjacent to p_a. Since $\pi_{T^*I_2} \circ u$ has degree zero near the intersection between the extensions of $(q_1'' q_b'')$ and $(q_2'' q_3'')$, $\dot{F}'_{(12)}$ cannot be a triangle. This leads to a contradiction. Therefore $\#\mathcal{M}^{\chi}(T_{w_1}, T_{w_2}, T_{w_3}) = 0$.

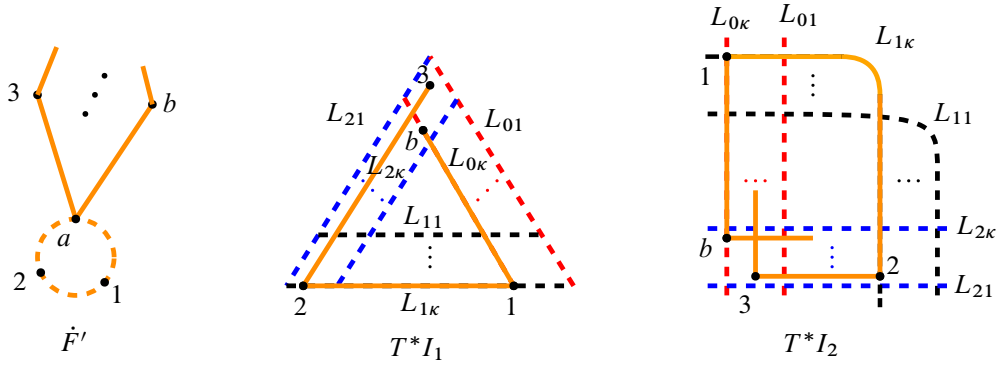

Figure 13: The case $t > \kappa - m$.

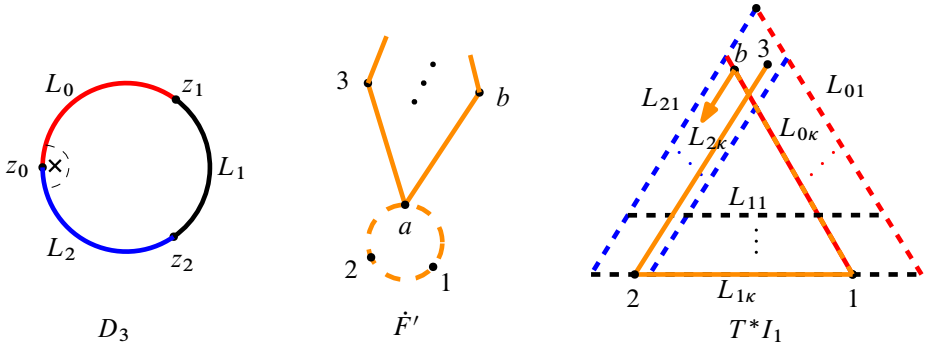

Figure 14: The case $t < \kappa - m$.

(3) $(t < \kappa - m)$ This case is shown in Figure 14. As $d \to 0$, $\dot{F}'_{(12)}$ bubbles off as a triangle with vertices $\{p_1, p_2, p_a\}$. On one hand, similar to the proof of $\#\mathcal{M}(T_{\mathrm{id}}, T_{\mathrm{id}}, T_1) = 0$ of Lemma 3.2, the projection of $\dot{F}'_{(b)}$ under $\pi_{D_3} \circ u$ is the constant map to z_0. On the other hand, the line denoted by the orange arrow is disjoint from L_{0i} for $i = 1, \dots, \kappa - 1$ since $(q'_1 q'_b)$ lies on $L_{0\kappa}$. So q'_b cannot be separated from the bottom left region. But the generators in this region are mapped to z_2 in the D_3-direction. We conclude that $\pi_{D_3} \circ u(\dot{F}'_{(b)})$ cannot be far from z_2. This is a contradiction. Therefore $\#\mathcal{M}^{\chi}(T_{w_1}, T_{w_2}, T_{w_3}) = 0$. □

The second case is when w_1 exchanges the last two elements. The schematic pictures are shown in Figures 15 and 16, which correspond to two subcases depending on the action of w_2 on the last two elements. The following proposition is a generalization of Lemmas 3.4 and 3.5:

Proposition 4.2 *For $w_1, w_2, w_3 \in S_\kappa$, suppose that $w_1 = w_1'' s_{\kappa-1}$, where $w_1'' \in S_{\kappa-2}$.*

(1) *If $w_2 = w_2'' s_{\kappa-2} \cdots s_{\kappa-m} s_{\kappa-1} s_{\kappa-2} \cdots s_{\kappa-l}$, where $w_2'' \in S_{\kappa-2}$ and $m > l \geq 0$, we have*

$$\#\mathcal{M}^{\chi}(T_{w_1}, T_{w_2}, T_{w_3}) = \begin{cases} \#\mathcal{M}^{\chi-2}(T_{w_1''}, T_{w_2''}, T_{w_3''}) & \text{if } w_3 = w_3'' s_{\kappa-1} s_{\kappa-2} \cdots s_{\kappa-m} s_{\kappa-1} s_{\kappa-2} \cdots s_{\kappa-l}, \\ 0 & \text{otherwise,} \end{cases}$$

where $w_3'' \in S_{\kappa-2}$.

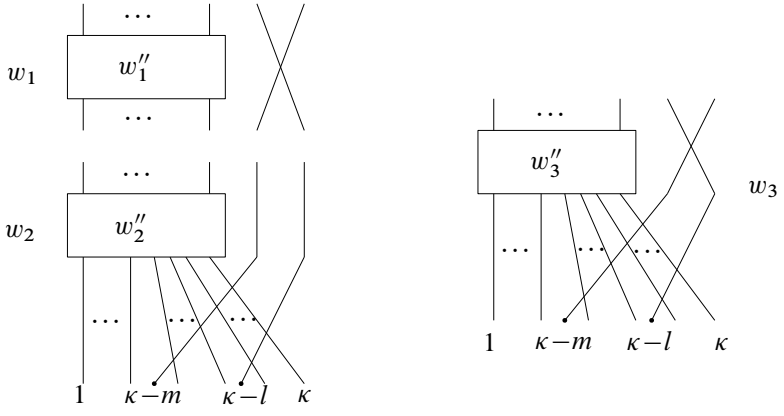

Figure 15: The case for Proposition 4.2(1).

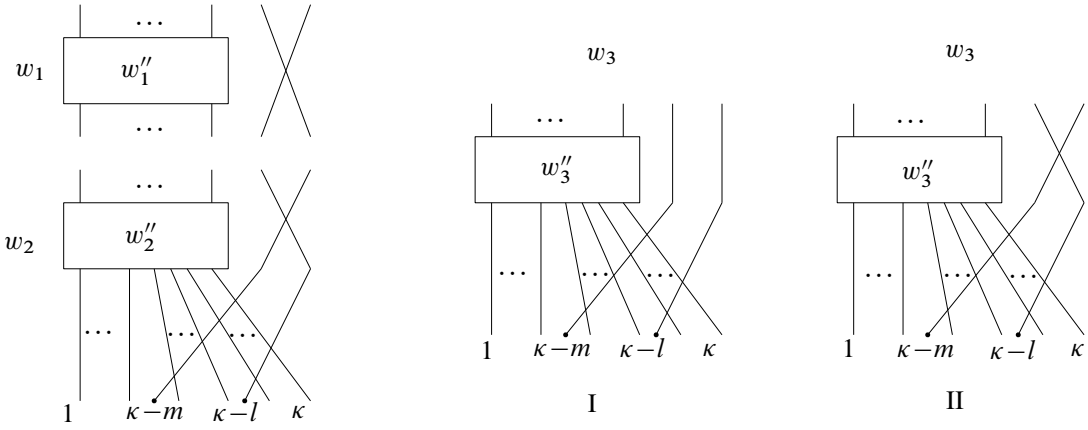

Figure 16: The case for Proposition 4.2(2).

(2) *If* $w_2 = w_2'' s_{\kappa-1} s_{\kappa-2} \cdots s_{\kappa-m} s_{\kappa-1} s_{\kappa-2} \cdots s_{\kappa-l}$, *where* $w_2'' \in S_{\kappa-2}$ *and* $m > l \geq 0$, *we have*

$$\#\mathcal{M}^{\chi}(T_{w_1}, T_{w_2}, T_{w_3}) = \begin{cases} \#\mathcal{M}^{\chi-2}(T_{w_1''}, T_{w_2''}, T_{w_3''}) & \text{if } w_3 = w_3'' s_{\kappa-2} \cdots s_{\kappa-m} s_{\kappa-1} s_{\kappa-2} \cdots s_{\kappa-l}, \\ \#\mathcal{M}^{\chi-1}(T_{w_1''}, T_{w_2''}, T_{w_3''}) & \text{if } w_3 = w_3'' s_{\kappa-1} s_{\kappa-2} \cdots s_{\kappa-m} s_{\kappa-1} s_{\kappa-2} \cdots s_{\kappa-l}, \\ 0 & \text{otherwise,} \end{cases}$$

where $w_3'' \in S_{\kappa-2}$.

Proof The proof is similar to but slightly longer than that of Proposition 4.1 since we need to discuss the last two strands of w_1 instead of one. We keep track of the following labels:

- the strands of w_3 which start from the positions κ and $\kappa-1$ end on positions t_1 and t_2, respectively,
- the strands of w_3 which end on the positions $\kappa-m$ and $\kappa-l$ start from positions r_1 and r_2, respectively.

Figure 17 describes the part of generators T_{w_1} and T_{w_2} corresponding to the last two strands of w_1, where the dashed circles describe the undetermined T_{w_3}. We discuss Cases 1 and 2 separately.

Case 1 ($t_1 = \kappa-m$ and $t_2 = \kappa-l$) This is equivalent to $w_3 = w_3'' s_{\kappa-1} s_{\kappa-2} \cdots s_{\kappa-m} s_{\kappa-1} s_{\kappa-2} \cdots s_{\kappa-l}$, for some $w_3'' \in S_{\kappa-2}$. Consider a holomorphic curve in $\mathcal{M}^{\chi}(T_{w_1}, T_{w_2}, T_{w_3})$ which contains two trivial

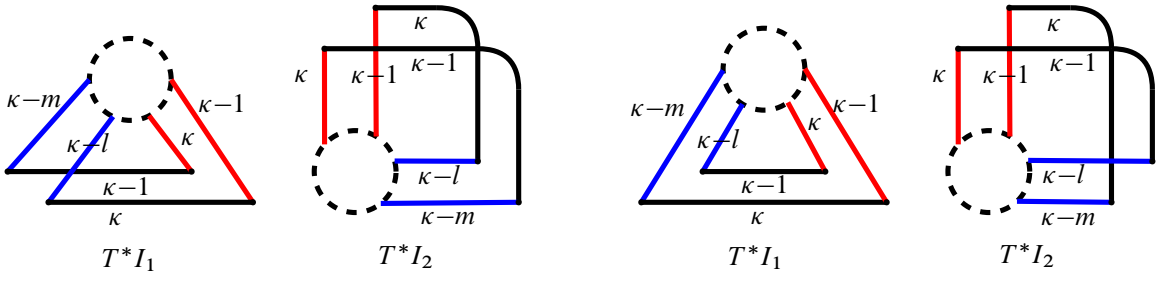

Figure 17: The part of generators T_{w_1} and T_{w_2} for Cases 1 (left) and 2 (right).

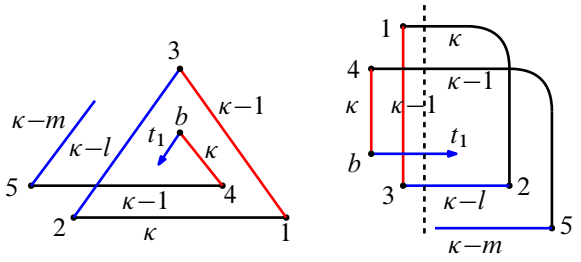

(i) $t_2 = k-l$ and $t_1 > k-l$

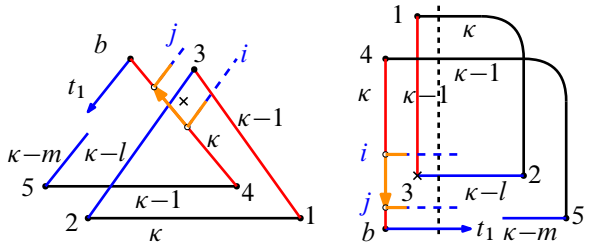

(ii) $t_2 = k-l$ and $t_1 < k-l$

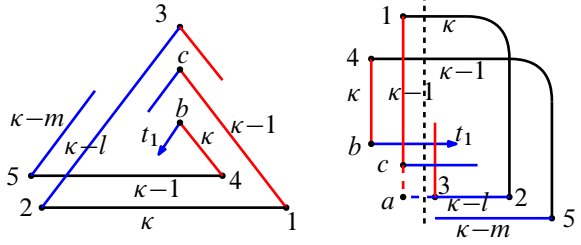

(iii) $t_2 > k-l$, $r_2 < k-1$ and $t_1 > k-l$

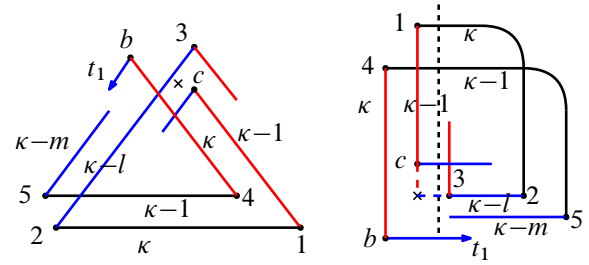

(iv) $t_2 > k-l$, $r_2 < k-1$ and $t_1 < k-l$

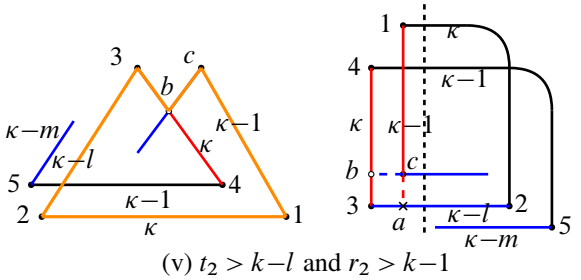

(v) $t_2 > k-l$ and $r_2 > k-l$

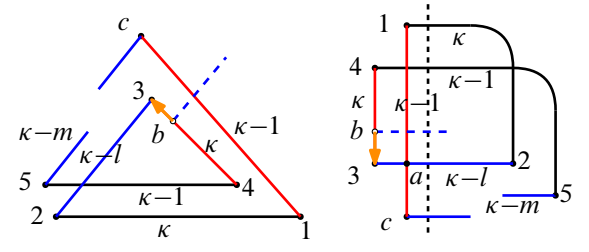

(vi) $t_2 < k-l$ and $r_2 > k-1$

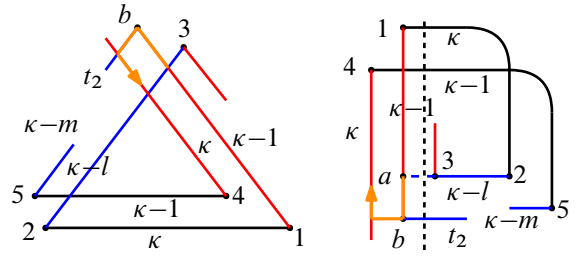

(vii) $t_2 < k-l$ and $r_2 < k-1$

Figure 18: The subcases of Case 1.

disks corresponding to the last two strands of w_1. The remaining components represent a curve in $\mathcal{M}^{\chi-2}(T_{w_1''}, T_{w_2''}, T_{w_3''})$. Thus $\mathcal{M}^{\chi-2}(T_{w_1''}, T_{w_2''}, T_{w_3''})$ can be viewed as a subset of $\mathcal{M}^{\chi}(T_{w_1}, T_{w_2}, T_{w_3})$. We show that no other curve exists in the rest of the proof. The subcases are shown in Figure 18.

(i) ($t_2 = k-l$ and $t_1 > k-l$) As $d \to 0$, $\dot{F}_{(12)}$ bubbles off as a triangle with vertices $\{p_1, p_2, p_a\}$, where $p_a \in \dot{F}'$ is the nodal point mapped to the limit of q_1' and q_2' in the T^*I_1-direction. Then the

projection of $\dot{F}'_{(3)}$ to the T^*I_2-direction must be the constant map to q''_3. Since $\pi_{T^*I_2}\circ u$ is of degree zero or one near q_3, the image $\pi_{T^*I_2}\circ u(\dot{F}\backslash(\dot{F}'_{(12)}\cup\dot{F}'_{(3)}))$ is disjoint from q''_3. This implies that $\dot{F}'_{(12)}\cup\dot{F}'_{(3)}$ is a connected component of $\dot{F}'$. Therefore the triangle $\{p_1, p_2, p_3\}$ forms a connected component of $\dot{F}$ before the degeneration. By removing the triangle $\{p_1, p_2, p_3\}$, the problem reduces to case (2) of the proof of Proposition 4.1 with $\kappa-1$ strands. Hence $\#\mathcal{M}^{\chi}(T_{w_1}, T_{w_2}, T_{w_3})=0$.

(ii) ($t_2=k-l$ and $t_1<k-l$) As $d\to 0$, $\dot{F}_{(12)}$ bubbles off as a triangle with vertices $\{p_1, p_2, p_a\}$ and the projection of $\dot{F}'_{(3)}$ to the T^*I_2-direction must be the constant map to q''_3. Moreover $\dot{F}'_{(3)}$ is a bigon with possible nodal degeneration points which are connected to other irreducible components of $\dot{F}'$. Denote one such nodal point on $\dot{F}'$ by p_n, whose images in T^*I_1 and T^*I_2 are drawn as the crossings in Figure 18(ii). We now remove the bigon $\dot{F}'_{(3)}$ from $\dot{F}'$ but keep p_n. We denote the irreducible component containing p_n in the remaining part of $\dot{F}'$ by $\dot{F}'_{p_n}$.

In the T^*I_2-direction, the projection of $u(\dot{F}'\backslash\dot{F}'_{(3)})$ to the left side of the vertical dotted line is of degree one. Let C be the boundary of the image $\pi_{T^*I_2}\circ(\dot{F}'_{p_n})$. Then the part of C near $L_{0\kappa}\cap L_{2(\kappa-l)}$ is locally drawn as the orange lines which go from L_{2i} to L_{2j} on $L_{0\kappa}$ for $i>\kappa-l$ and $j<\kappa-m$. We denote the preimage of the orange arrow from L_{2i} to L_{2j} by C_{arrow}. It has the positive boundary orientation.

In the T^*I_1-direction, the position of the crossing must be above $L_{0\kappa}$ since $\pi_{D_3}\circ u(p_n)=z_0$. However, the image of C_{arrow}, denoted by the orange arrow, has the negative boundary orientation. This leads to a contradiction. Therefore $\#\mathcal{M}^{\chi}(T_{w_1}, T_{w_2}, T_{w_3})=0$.

(iii) ($t_2>k-l$, $r_2<k-1$ and $t_1>k-l$) As $d\to 0$, $\dot{F}_{(12)}$ bubbles off as a triangle with vertices $\{p_1, p_2, p_a\}$. Since on T^*I_2, $\pi_{T^*I_2}\circ u$ is of degree zero near the intersection of the extension of $(q''_1q''_c)$ and $(q''_2q''_3)$, $\{p_1, p_2, p_a\}$ cannot form a triangle. This leads to a contradiction. Therefore $\#\mathcal{M}^{\chi}(T_{w_1}, T_{w_2}, T_{w_3})=0$.

(iv) ($t_2>k-l$, $r_2<k-1$ and $t_1<k-l$) As $d\to 0$, $\dot{F}_{(12)}$ bubbles off as a triangle with vertices $\{p_1, p_2, p_a\}$, where p_a is mapped to a point in T^*I_2, denoted by a crossing. We denote the preimage of this crossing in the irreducible component other than $\dot{F}_{(12)}$ and $\dot{F}_{(3)}$ by p_n. The image of p_n in T^*I_1 is also denoted by a crossing. It sits above $L_{0\kappa}$ for the same reason as in (ii). The remaining argument is the same as in (ii). We conclude that $\#\mathcal{M}^{\chi}(T_{w_1}, T_{w_2}, T_{w_3})=0$.

(v) ($t_2>k-l$ and $r_2>k-1$) As $d\to 0$, $\dot{F}_{(12)}$ bubbles off as a triangle T with vertices $\{p_1, p_2, p_a\}$, where p_a is mapped to the crossing in T^*I_2. The other irreducible component of $\dot{F}'$ containing p_a is the quadrilateral Q with vertices $\{p_3, p_c, p_a, p_b\}$, which is the bottom-left part in the T^*I_2-direction. Figure 19 describes the degenerated domain $\dot{F}'$.

Removing T and Q from $\dot{F}'$ corresponds to removing the orange polygon in the T^*I_1-direction. As a result, the vertices $\{p_1, p_2, p_3, p_c\}$ are replaced by p_b. Then the problem is reduced to case (2) of the proof of Proposition 4.1 with $\kappa-1$ strands. Hence, $\#\mathcal{M}^{\chi}(T_{w_1}, T_{w_2}, T_{w_3})=0$.

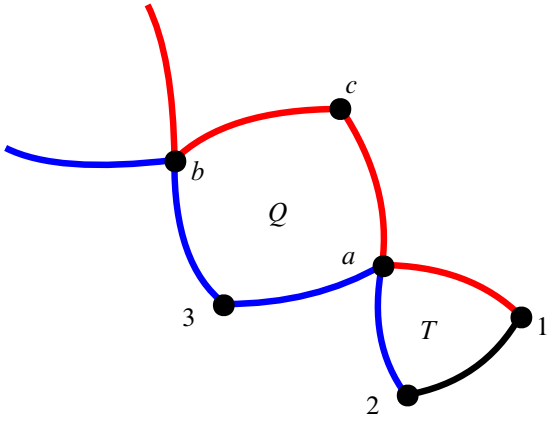

Figure 19: The subcase (v).

(vi) ($t_2 < k-l$ and $r_2 > k-1$) This is similar to (ii). The orientation of the orange arrows leads to a contradiction. Hence $\#\mathcal{M}^{\chi}(T_{w_1}, T_{w_2}, T_{w_3}) = 0$.

(vii) ($t_2 < k-l$ and $r_2 < k-1$) This is similar to (ii). So $\#\mathcal{M}^{\chi}(T_{w_1}, T_{w_2}, T_{w_3}) = 0$.

Case 2 The subcases are shown in Figure 20. The proofs of all subcases are similar to those in Case 1 except for (v). We discuss (v) only and omit the others.

(v) ($t_2 > k-m$ and $r_1 > k-1$) The proof is similar to that of subcase (v) of Case 1. As $d \to 0$, $\dot{F}_{(12)}$ bubbles off as a triangle T with vertices $\{p_1, p_2, p_a\}$, where p_a is mapped to the crossing in T^*I_2, and $\{p_3, p_c, p_a, p_b\}$ forms a quadrilateral Q, as the bottom-left part in the T^*I_2-direction. Figure 19 describes the degenerated domain $\dot{F}'$. Removing T and Q from $\dot{F}'$ corresponds to removing the orange polygon in the T^*I_1-direction. As a result, the vertices $\{p_1, p_2, p_3, p_c\}$ are replaced by p_b. Then the problem is reduced to the case with $\kappa - 1$ strands. There are three possibilities:

(a) ($t_2 = \kappa - l$) This is similar to (1) in the proof of Proposition 4.1. If the limiting curve exists, then $\{p_1, p_2, p_3, p_4, p_5, p_c\}$ must forms a (hexagon) disk component H of $\dot{F}$. The count of $u \in \mathcal{M}^{\chi}(T_{w_1}, T_{w_2}, T_{w_3})$ restricted to H is exactly the count of $\mathcal{M}^{\chi=1}(T_1, T_1, T_1)$ in Lemma 3.5, which is equals one. The count of u restricted to $\dot{F}\backslash H$ is the count of $\mathcal{M}^{\chi-1}(T_{w_1''}, T_{w_2''}, T_{w_3''})$. Therefore $\#\mathcal{M}^{\chi}(T_{w_1}, T_{w_2}, T_{w_3}) = \#\mathcal{M}^{\chi-1}(T_{w_1''}, T_{w_2''}, T_{w_3''})$.

(b) ($t_2 > \kappa - l$) This is similar to (2) in the proof of Proposition 4.1. So $\#\mathcal{M}^{\chi}(T_{w_1}, T_{w_2}, T_{w_3}) = 0$.

(c) ($t_2 < \kappa - l$) This is similar to (3) in the proof of Proposition 4.1. So $\#\mathcal{M}^{\chi}(T_{w_1}, T_{w_2}, T_{w_3}) = 0$. □

The following corollaries are direct consequences by inductively using the two propositions above.

Corollary 4.3 *The generator T_{id} is the identity in* $\mathrm{End}(L^{\otimes\kappa})$.

Corollary 4.4
$$T_i T_w = \begin{cases} T_{s_i w} & \text{if } l(s_i w) > l(w), \\ T_{s_i w} + \hbar T_w & \text{if } l(s_i w) < l(w). \end{cases}$$

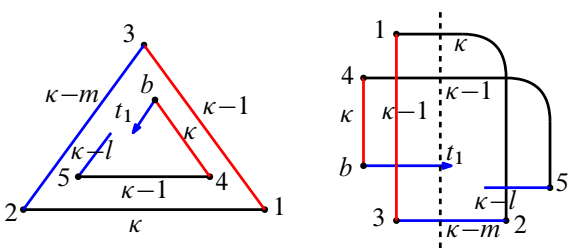

(i) $t_2 = k-m$ and $t_1 > k-m$

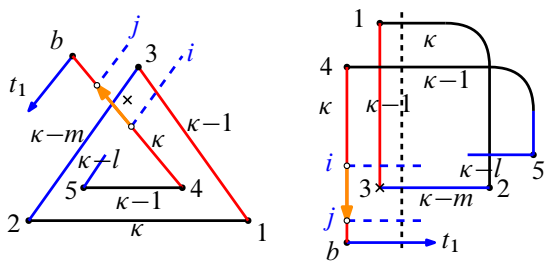

(ii) $t_2 = k-m$ and $t_1 < k-m$

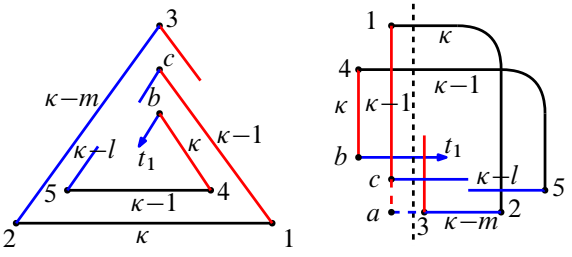

(iii) $t_2 > k-m$, $r_1 < k-1$ and $t_1 > k-m$

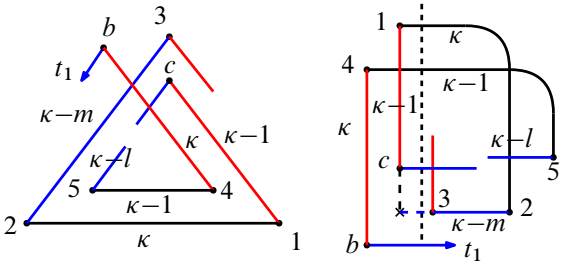

(iv) $t_2 > k-m$, $r_1 < k-1$ and $t_1 < k-m$

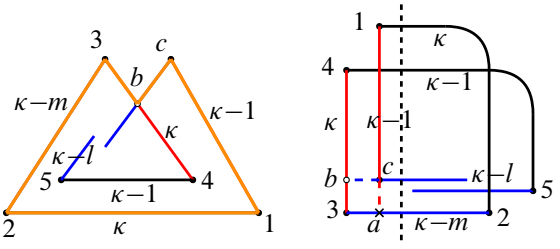

(v) $t_2 > k-m$ and $r_1 > k-1$

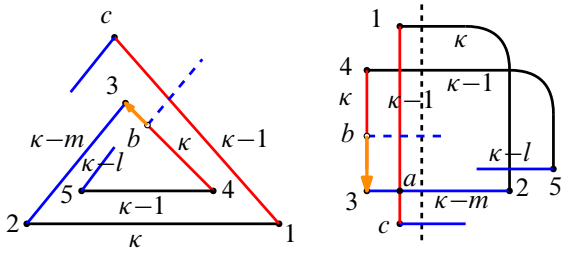

(vi) $t_2 < k-m$ and $r_1 > k-1$

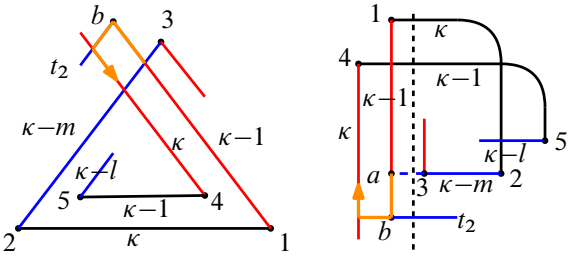

(vii) $t_2 < k-m$ and $r_1 < k-1$

Figure 20: The subcases of Case 2.

Corollary 4.5 *The generators T_i satisfy the relations in the Hecke algebra*

$$T_i^2 = 1 + \hbar T_i, \tag{4-1}$$

$$T_i T_j = T_j T_i \quad \text{for } |i-j| > 1, \tag{4-2}$$

$$T_i T_{i+1} T_i = T_{i+1} T_i T_{i+1}. \tag{4-3}$$

Proof of Theorem 1.2 Define a unital $\mathbb{Z}[\hbar]$-algebra map $\phi\colon H_\kappa \to \mathrm{End}(L^{\otimes\kappa})$ on the algebra generators by $\phi(\widetilde{T}_i) = T_i$. The map is well defined by Corollary 4.5. The multiplication rules on H_κ in (1-1) and that of $\mathrm{End}(L^{\otimes\kappa})$ in Corollary 4.4 are the same. So $\phi(\widetilde{T}_w) = T_w$ for all $w \in S_\kappa$. □

References

[1] **A Abbondandolo**, **M Schwarz**, *Floer homology of cotangent bundles and the loop product*, Geom. Topol. 14 (2010) 1569–1722 MR Zbl

[2] **M Abouzaid**, *On the wrapped Fukaya category and based loops*, J. Symplectic Geom. 10 (2012) 27–79 MR Zbl

[3] **V Colin**, **K Honda**, **Y Tian**, *Applications of higher-dimensional Heegaard Floer homology to contact topology*, J. Topol. 17 (2024) art. id. e12349 MR Zbl

[4] **T Ekholm**, **V Shende**, *Skeins on branes*, preprint (2019) arXiv 1901.08027

[5] **S Ganatra**, **J Pardon**, **V Shende**, *Covariantly functorial wrapped Floer theory on Liouville sectors*, Publ. Math. Inst. Hautes Études Sci. 131 (2020) 73–200 MR Zbl

[6] **S Ganatra**, **J Pardon**, **V Shende**, *Sectorial descent for wrapped Fukaya categories*, J. Amer. Math. Soc. 37 (2024) 499–635 MR Zbl

[7] **K Honda**, **Y Tian**, **T Yuan**, *Higher-dimensional Heegaard Floer homology and Hecke algebras*, J. Eur. Math. Soc. (online publication August 2024)

[8] **V F R Jones**, *Hecke algebra representations of braid groups and link polynomials*, Ann. of Math. 126 (1987) 335–388 MR Zbl

[9] **H R Morton**, **P Samuelson**, *DAHAs and skein theory*, Comm. Math. Phys. 385 (2021) 1655–1693 MR Zbl

[10] **Z Sylvan**, *On partially wrapped Fukaya categories*, J. Topol. 12 (2019) 372–441 MR Zbl

School of Mathematical Sciences, Beijing Normal University
Beijing, China

School of Mathematical Sciences, Eastern Institute of Technology, Ningbo
Zhejiang, China

yintian@bnu.edu.cn, tyyuan@eitech.edu.cn

Received: 24 August 2023 Revised: 24 November 2023

ALGEBRAIC & GEOMETRIC TOPOLOGY

msp.org/agt

See inside back cover or msp.org/agt for submission instructions.

The subscription price for 2025 is US $760/year for the electronic version, and $1110/year (+$75, if shipping outside the US) for print and electronic. Subscriptions, requests for back issues and changes of subscriber address should be sent to MSP. Algebraic & Geometric Topology is indexed by Mathematical Reviews, Zentralblatt MATH, Current Mathematical Publications and the Science Citation Index.

Algebraic & Geometric Topology (ISSN 1472-2747 printed, 1472-2739 electronic) is published 9 times per year and continuously online, by Mathematical Sciences Publishers, c/o Department of Mathematics, University of California, 798 Evans Hall #3840, Berkeley, CA 94720-3840. Periodical rate postage paid at Oakland, CA 94615-9651, and additional mailing offices. POSTMASTER: send address changes to Mathematical Sciences Publishers, c/o Department of Mathematics, University of California, 798 Evans Hall #3840, Berkeley, CA 94720-3840.

AGT peer review and production are managed by EditFlow® from MSP.

PUBLISHED BY

mathematical sciences publishers

nonprofit scientific publishing

https://msp.org/

ALGEBRAIC & GEOMETRIC TOPOLOGY

Volume 25 Issue 3 (pages 1265–1915) 2025